10146 *Inorg. Chem.* **2009**, *48*, 10146–10150
DOI: 10.1021/ic901085p

Inorganic Chemistry
Article

Magneto−Structural Correlation in a Metamagnetic Cobalt(II)-Based Pillared Trilayer Motif Constructed by Mixed Pyridyl-Type Carboxylate Ligands

Yan-Ling Zhou,[†,‡] Mei-Chun Wu,[†] Ming-Hua Zeng,*[,†] and Hong Liang*[,†,‡]

[†]*Key Laboratory for the Chemistry and Molecular Engineering of Medicinal Resources (Ministry of Education of China), School of Chemistry & Chemical Engineering, Guangxi Normal University, Guilin 541004, P. R. China, and* [‡]*Department of Chemistry and Chemical Engineering, Central South University, Changsha 410083, P. R. China*

Received June 5, 2009

The first structurally authenticated example of coordinated polymer featuring homometallic pillared-trilayer structure, $[Co_3(ina)_2(pico)_2(H_2O)_2]_n$ (**1**), was built from mixed pyridyl-type monocarboxylates, isonicotinate (ina) and 3-hydroxypicolinate (pico), containing Kagomé-type $[Co_3(pico)_2(H_2O)_2]_n^{2n+}$ trilayers. The magnetic phase diagram of **1** shows a metamagnetic transition below 3.2 K, arising from the competing interactions between the antiferromagnetic intralayer couplings in different amplitudes with obviously noncompensated moments versus weak AF interlayer coupling.

Introduction

In molecular magnetism, a few magnetically ordered complexes exhibit metamagnetic phase transitions,[1,2] and most of them are heterometallic[3] or homometallic compounds[4] or metal-radical materials[5] that display low dimensionality (1D or 2D) structures. In particular, homometallic 3D metamagnets have been documented in several azide-bridged complexes[6] and metal phosphonates[7] or metal carboxylates.[8] As well-known, complicated magnetic anisotropy has significant influence on the metamagnetism, and coupling of the magnetic ordering is a consequence of the 3D structure. So far the design of polynuclear metal complexes and extended networks with predictable magnetic properties is still a challenge in the field of molecular magnetism. A great deal of work is required to understand the structural factors that govern the exchange coupling between paramagnetic centers, since such a relationship is complex and remains elusive.[1,9] 3D frameworks built by pillared layers provide an opportunity for systematical study of the relationship between the structure and metamagnetic properties for the exchange between the layers mediated by pillars are always AF but weak and thus readily overcome by the applied field.[10] Furthermore, the "organic" layers in pillared layered

*To whom correspondence should be addressed. E-mail: zmh@mailbox.gxnu.edu.cn. Fax: 86 773 2120-958.

(1) (a) Batten, S. R.; Neville, S. M.; Turner, D. R. *Coordination Polymers Design, Analysis and Application*; The Royal Society of Chemistry: 2009. p 273-372. (b) Zeng, Y.-F.; Hu, X.; Liu, F.-C.; Bu, X.-H. *Chem. Soc. Rev.* **2009**, *38*, 469.

(2) (a) Gao, E.-Q.; Liu, P.-P.; Wang, Y.-Q.; Yue, Q.; Wang, Q.-L. *Chem. Eur. J.* **2009**, 1217. (b) Zeng, M.-H.; Zhang, W.-X.; Sun, X.-Z.; Chen, X.-M. *Angew. Chem., Int. Ed.* **2005**, *44*, 3079.

(3) (a) Kwak, S. C.; W, Yoon, H. Y.; Kim, J. H.; Koh, H. C.; Hong, C. S. *Inorg. Chem.* **2008**, *47*, 10214. (b) Wang, X.-Y.; Wang, Z.-M.; Gao, S. *Chem. Commun.* **2008**, 281.

(4) (a) Jia, H.-P.; Li, W.; Ju., Z.-F.; Zhang, J. *Chem. Commun.* **2008**, 371. (b) Zheng, Y.-Z.; Xue, W.; Tong, M.-L.; Chen, X.-M.; Grandjean, F. *Inorg. Chem.* **2008**, *47*, 4077. (c) Tao, J.; Zhang, Y.-Z.; Bai., Y.-L.; Sato, O. *Inorg. Chem.* **2006**, *45*, 4877.

(5) (a) Ishii, N.; Okamura, Y.; Chiba, S.; Nogami, T.; Ishida, T. *J. Am. Chem. Soc.* **2008**, *130*, 24. (b) Aoki, C.; Ishida, T. *Inorg. Chem.* **2003**, *42*, 7616. (c) Numata, Y.; Inoue, K.; Baranov, N.; Kurmoo, M.; Kikuchi, K. *J. Am. Chem. Soc.* **2007**, *129*, 9902.

(6) (a) Mondal, K. C.; Mukherjee, P. S. *Inorg. Chem.* **2008**, *47*, 4215. (b) Gao, E.-Q.; Wang, Z.-M.; Yan, C.-H. *Chem. Commun.* **2003**, 1748.

(7) (a) Yang, T.-H.; Liao, Y.; Zheng, L. M.; Dinnebier, R. E.; Su, Y.-H.; Ma, J. *Chem. Commun.* **2009**, 3023. (b) Chang, W. K.; Chiang, R. K.; Jiang, Y. C.; Wang, S. L.; Lee, S. F.; Li, K. H. *Inorg. Chem.* **2004**, *43*, 2564. (c) Yin, P.; Gao, S.; Zheng, L.-M.; Wang, Z.-M.; Xin, X.-Q. *Chem. Commun.* **2003**, 1076. (d) Rabu, P.; Janvier, P.; Bujoli, B. *J. Mater. Chem.* **1999**, *9*, 1323.

(8) (a) Wang, X.-Y.; Sevov, S. C. *Inorg. Chem.* **2008**, *47*, 1037. (b) Demessence, A.; Rogez, G.; Rabu, P. *Chem. Mater.* **2006**, *18*, 3005. (c) Wang, X.-Y.; Wang, L.; Wang, Z. M.; Su, G.; Gao, S. *Chem. Mater.* **2005**, *17*, 6369. (d) Feyerherm, R.; Loose, A.; Rabu, P.; Drillon, M. *J. Solid State Chem.* **2003**, *5*, 321. (e) Huang, Z.-L.; Drillon, M.; Masciocchi, N.; Sironi, A.; Zhao, J.-T.; Rabu, P.; Panissod, P. *Chem. Mater.* **2000**, *12*, 2805.

(9) (a) Zeng, M.-H.; Wu, M.-C.; Liang, H.; Zhou, Y.-L.; Chen, X.-M.; Ng, S. W. *Inorg. Chem.* **2007**, *46*, 7241. (b) Yao, M.-X.; Zeng, M.-H.; Zou, H.-H.; Zhou, Y.-L.; Liang, H. *Dalton Trans.* **2008**, 2428. (c) Zeng, M.-H.; Feng, X.-L.; Zhang, W.-X.; Chen, X.-M. *Dalton Trans.* **2006**, 5294. (d) Zeng, M.-H.; Wang, B.; Wang, X. Y.; Zhang, W.-X.; Chen, X.-M.; Gao, S. *Inorg. Chem.* **2006**, *45*, 7069. (e) Zhou, Y.-L.; Meng, F.-Y.; Zhang, J.; Zeng, M.-H.; Liang, H. *Crystal Growth Des.* **2009**, *9*, 1402. (f) Zeng, M.-H.; Yao, M.-X.; Liang, H.; Zhang, W.-X.; Chen, X.-M. *Angew. Chem., Int. Ed.* **2007**, *46*, 1832.

(10) (a) Chang, W. K.; Chiang, R. K.; Jiang, Y. C.; Wang, S. L.; Lee, S. F.; Li, K. H. *Inorg. Chem.* **2004**, *43*, 2564. (b) Yin, P.; Zheng, L.-M.; Gao., S.; Xin, X.-Q. *Chem. Commun.* **2001**, 2346. (c) Hao, X.; Wei, Y.-G.; Zhang, S.-W. *Chem. Commun.* **2000**, 2271. (c) Hou, S.-Z.; Cao, D.-K.; Liu, X.-G.; Li, Y.-Z.; Zheng, L.-M. *Dalton Trans.* **2009**, 2746. (d) Shiga, T.; kawa, H.; Kitagawa, S.; Ohba, M. *J. Am. Chem. Soc.* **2006**, *128*, 16426. (e) Gao, E.-Q.; Cheng, A.-L.; Xu, Y.-X.; He, M.-Y.; Yan, C.-H. *Inorg. Chem.* **2005**, *44*, 8822.

Published on Web 09/30/2009

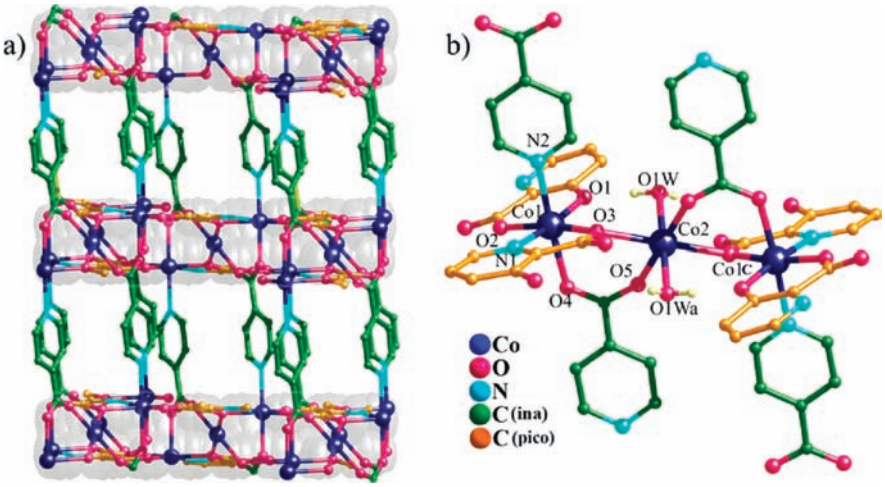

Figure 1. (a) Plot of a 3D pillar-trilayered structure of **1** along the *b* axis (left). (b) Plot of the Co(II) coordinated environments showing the pico bridges within the trimer in **1**. Some H atoms are omitted for clarity.

coordination polymer may be of the so far widely observed, but theoretically important 2D spin topologies and spin-frustrated lattices, such as the Kagomé or triangle lattice.[11] Such geometrically frustrated antiferromagnetic materials have attracted much attention in recent years because of their propensity to adopt unusual, even exotic, magnetic ground states which remain poorly understood.[12,13]

In our previous work, we have reported a rare interpenetrating 3D structure $[Co_4(pico)_4(4,4'\text{-bpy})_3(H_2O)_2]_n \cdot 2nH_2O$,[2b] in which pico was chosen as a bischelating ligand to construct alternating 1D chains of Co(II) ions (Scheme S1, mode II), owing to the predictable asymmetrical exchanging modes of pico ligands. As a result, the strong anisotropy from single ions arranged in the chains, sheets, and finally, the 3D structure were controlled, and a typical metamagnet was acquired. Encouraged by previous results, we also chose pico ligand and introduced multifunctional ina to replace 4,4′-bpy coligand. For the various coordination modes adopted by the ina linkers, some new complicated networks with predictable magnetic properties will be acquired.[9a−c] Herein, we describe typically metamagnetic behavior of a unique 3D pillared Kagomé-type trilayer motif, $[Co_3(ina)_2(pico)_2(H_2O)_2]_n$, (Figure 1a), constructed from above mixed pyridyl-type monocarboxylate ligands.

Experimental Section

Materials and Physical Measurements. The reagents and solvents employed were commercially available and used as received without further purification. The C, H, and N microanalyses were carried out with an Elementar Vario-EL CHNS elemental analyzer. The FT-IR spectra were recorded from KBr pellets in the range 4000− 400 cm^{-1} on a Bio-Rad FTS-7 spectrometer. Temperature and field-dependent magnetic measurements were carried out on a SQUID-MPMS-XL-7 magnetometer. Diamagnetic corrections were made with Pascal's constants.

Synthesis of 1. Complex **1** was prepared from H_2pico (0.139 g, 1 mmol) in an aqueous solution (6 mL) of NaOH (0.080 g, 2 mmol) was mixed with ina (0.092 g, 0.75 mmol) in EtOH (2 mL), which was then added to an aqueous solution (2 mL) of $Co(NO_3)_2 \cdot 6H_2O$ (0.291 g, 1 mmol). The mixture was placed in a 23-mL Teflon-lined autoclave and heated at 150 °C for 48 h. The autoclave was cooled over a period of 12 h at a rate of 5 °C h^{-1}, and **1**, as red crystals, was collected by filtration, washed with water, and dried in air. The phase-pure **1** was obtained by manual separation (final yield = 16% based on Co). Elemental analyses: calcd (%) for **1** C, 39.42, H, 2.48, N, 7.66; found (%) C, 40.01, H, 3.01, N, 7.50. IR data (λ, cm^{-1}): 3477 *s*, 2816 *m*, 1619 vs, 1597 *s*, 1567 *s*, 1545 *s*, 1468 *m*, 1416 *m*, 1396 *m*, 1244 *s*, 1154 *m*, 1123 *m*, 1062 *m*, 911 *m*, 778 *m*, 706 *m*, 599 *m*.

Table 1. Summary of Crystallographic Data for **1**

compound	**1**
empirical formula	$C_{24}H_{18}Co_3N_4O_{12}$
fw	731.21
cryst syst	monoclinic
space group	$P2_1/c$
a/Å	9.323(2)
b/Å	12.212(2)
c/Å	11.736(2)
β/°	93.588(4)
V/Å^3	1333.6(4)
Z	2
D_c/g·cm^{-3}	1.821
abs coeff (mm^{-1})	1.917
F (000)	734
reflns collected, independent	2904, 2098
R1/wR2 [$I > 2\sigma(I)$]	0.0340/0.0676
GOF on F^2	1.050
largest diff. peak and hole (e Å^{-3})	0.424/−0.377

X-ray Crystallography. Diffraction data were collected on a Bruker Smart Apex CCD diffractometer with graphite monochromated Mo Kα radiation (λ = 0.71073 Å), and the absorption corrections were applied by SADABS.[14] The structures were solved by direct methods and refined using full-matrix least-squares technique with SHELXL-97.[14] Experimental details of the X-ray analyses are provided in Table 1. Selected bond distances and angles are listed in Table S1, Supporting Information.

Results and Discussion

Crystal Structure. Single-crystal X-ray diffraction shows that **1** features a pillared trilayer 3D motif, consisting

(11) For example, see: (a) Kanoo, P.; Madhu, C.; Mostafa, G.; Maji, T. K.; Sundaresan, A.; Pati, S. K.; Rao, C. N. R. *Dalton Trans.* **2009**, 5062. (b) Wang, X.-Y.; Wang, L.; Wang, Z.-M.; Gao, S. *J. Am. Chem. Soc.* **2006**, *128*, 674. (c) Zheng, Y.-Z.; Tong, M.-L.; Zhang, W.-X.; Chen, X.-M. *Chem. Commun.* **2006**, 165.

(12) Greedan, J. E. *J. Mater. Chem.* **2001**, *11*, 37.

(13) Pati, S. K.; Rao, C. N. R. *Chem. Commun.* **2008**, 4683.

(14) (a) Sheldrick, G. M. *SADABS 2.05*, University Göttingen; Göttingen, Germany. (b) *SHELXTL 6.10*; Bruker Analytical Instrumentation: Madison, WI, 2000.

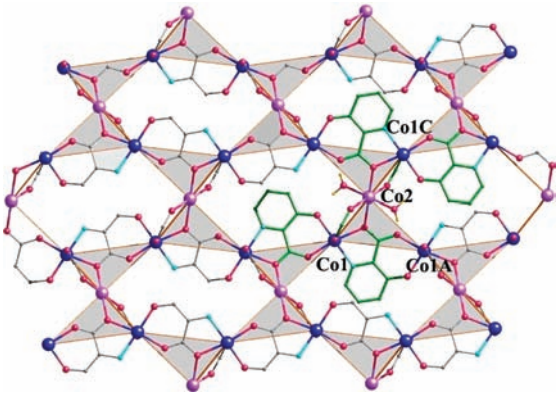

Figure 2. 2D pseudo-Kagomé sheet and (single oxygen atom-bridged Co···Co edges shown as bold lines; those not involving significant magnetic interactions shown as thin lines) in the structure of $[Co_3(pico)_2(H_2O)_2]_n^{2n+}$ along *c* direction. The highlighted section shows two syn−syn and μ_2-O carboxylate bridges from ina and pico in trimer. Some coordinated water molecules, C atoms of pico, and H atoms are omitted for clarity.

of linear trinuclear Co(II) subunits connected via ina and pico ligands (Figure 1). The outer Co1 atom is bichelated by O,N-chelating and O,O′-chelating sites of two adjacent pico ligands and the slightly distorted six coordination geometry is completed by one pyridyl N atom, one carboxylate O atom from ina ligand [Co1−O = 2.002(2)−2.129(2) Å; Co1−N = 2.080(2)−2.182(3) Å]. The central Co2 atom is linked to two terminal Co1 atoms with mixed bridges through one trans-related carboxyl oxygen atom from pico group and one syn−syn 1,3-carboxylate from ina groups (Co2−O3 = 2.195(2) Å, Co2−O5 = 2.041(2) Å, Co1···Co2 = 3.707 Å, Co1−O3−Co2 118.0(9)°) to form a trimer, and the remaining two (axial) positions around Co2 are occupied by terminal water molecules (Co2−O1W = 2.093(2) Å). Each trimer is linked with four adjacent trimers by pico groups through μ_3-κN,O:κO-μ_2:κO′,O″ bridging mode (Scheme S1, mode II, Supporting Information), resulting in a thickness of distorted Kagomé-type trilayer motif only 2.6 Å along the *b* axis, $[Co_3(pico)_2(H_2O)_2]_n^{2n+}$ (Figure 2). The resulting topological lattice is different from a standard Kagomé lattice not only because the Co(II) atoms are not in the same plane along the *b* axis but also because not all the Co(II) atoms are corner-shared.[11−13]

In alternative way, the special layer consists of infinite zigzag chains of $[Co(pico)]_n$ (Co1···Co1A 5.916 Å) along the *c*-axis, and further paralleled linked by Co2 octahedras (Co2···Co1A = 5.186 Å). The layer can also be simply described as a rigid honeycomb network, in which every eight Co(II) are interconnected to form a hexagon ring. Notably, the above trilayer is quite different from that of our previously reported manganese succinate or cobalt malate layer structure pillared by ina spacers, with a single metallic layer,[8a,c] and also distinct from that of Li et al. reported a heterometallic Na(I)−Co(II)−Na(I) trilayer pillared by biphenyldicarboxylate,[15] which represents the first example of a Co(II) based Kagomé-type trilayer interconnected uniquely by carboxylate groups without the presence of any hydroxyl groups. Such unique layer mainly arises from the bridging pico ligand having asymmetrical O,N-chelating (forming a five-member ring) and O,O′-chelating (forming a six-member ring).

The unique layers in **1** are cross-pillared by μ_3-ina ligands with exotridentate bridging mode to form a 3D structure in an AA packing mode. The interlayer distance is ~6.7 Å, and evidently shorter than that of ina pillared manganese succinate (9.23 Å) or cobalt malate layer (9.09 Å).[8a,c] The ina pillars of **1** with twisting (the torsion angle of the fragments of C7−O4−O5−Co2 and C7−O4−O5−Co1 are −158.77 and −177.67, respectively) are a result of orientation adjustment to achieve stable coordination geometry for the metal ions from adjacent declining layers. Hence, the closely packed and tilting ina pillars within **1** are too close to accommodate guest solvent molecules. Obviously, the occurrence of mutual structure-directing effects of a fascinating packing style pillared trilayer structure in the **1** may be attributed to shape, size, and coordination recognition between the mixed pyridyl-type monocarboxylates ligands.[16] Hydrogen-bonding interactions are present within the 3D motif. The coordinated water molecules participate in very strong hydrogen bonds within trimer (O1W···O1 = 2.578 Å) and moderate hydrogen bonds (O1W···O2 = 2.868 Å; O1W···O4 = 3.171 Å), with oxygen atoms of carboxyl group from pico and ina of neighboring trimer, respectively (Figure S1 and Table S1, Supporting Information).

Topologically, the Co(II) trimers can be regarded as the network nodes. These are linked in two dimensions by the pico ligands to give (4,4) sheets. The 2D sheets are further connected by pairs of ina ligands coordinating to the trinuclear SBUs to form a 3D framework with six-connected pcu topology. Although lots of complexes with pcu topology have been reported, they all contain only one kind of edges (all single or all double).[16c,17] However, this unusual 6-connected SBU make the present pcu contain both single and double edges.

Magnetic Studies. Magnetic susceptibility measurements carried out on crushed single crystals of **1** with 1 kOe. The $\chi_m T$ product of each Co_3 unit (9.32 cm^3 K mol^{-1}) at 300 K is in agreement with that expected for three magnetically isolated high-spin Co(II) atoms with $S = 3/2$, exhibiting strong spin−orbit coupling (Figure 3).[9] First, it exhibits a monotonic decrease in $\chi_m T$ until a minimum (4.50 cm^3 K mol^{-1}) at 7.5 K with decreasing temperature, then an increase upon further lowering of the temperature, a peak (8.60 cm^3 K mol^{-1}) at 3.2 K, and finally a rapid decrease to a value of 1.25 cm^3 K mol^{-1} at 2 K, indicating a ferrimagnetic like behavior, although spin−orbit coupling effect could not be ruled out. The magnetic susceptibility above 60 K obeys the Curie−Weiss law very well (Figures 3 and S3, Supporting Information), giving a Curie constant *C* of 10.1 cm^3 mol^{-1} K and a Weiss constant θ of −24.6 K. This fact

(15) Pan, L.; Finkel, B. S.; Huang, X.-Y.; Li, J. *Chem. Commun.* **2001**, 105.

(16) (a) Rotello, V.; Thayumanavan, S. *Molecular Recognition and Polymers: Control of Polymer Structure. Self-Assembly*; Willey-VCH: Weinheim, Germany, 2008. (b) Hu, S.; Zou, H.-H.; Zeng, M.-H.; Wang, Q.-X.; Liang, H. *Cryst. Growth Des.* **2008**, *8*, 2346. (c) Chen, Q.; Zhou, Y.-L.; Zeng, M.-H. *J. Mol. Struct.* **2009**, *932*, 55.

(17) (a) Öhrström, L.; Larsson, K. *Molecule-Based Materials The Structural Network Approach*; Elsevier, 2005; p 96. (b) Zeng, M.-H.; Liu, Z.-T.; Zou, H.-H.; Liang, H. *J. Mol. Struct.* **2007**, *828*, 75.

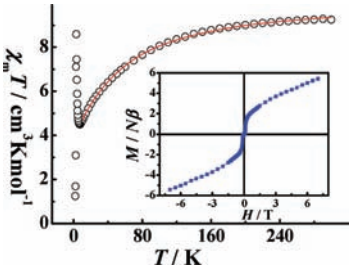

Figure 3. Temperature dependence of $\chi_m T$ for **1** measured at 1 kOe. The solid line represents the best fit given in the text. The inset shows magnetization plot at 2 K.

indicates the antiferromagnetic coupling between the Co(II) ions.

To understand the high temperature behavior, the noncritical-scaling theory with the following simple phenomenological equation was used to fit the experimental data from 300 to 10 K:[18]

$$\chi T = A \exp(-E_1/kT) + B \exp(-E_2/kT)$$

Here, $A + B$ equals the Curie constant, and E_1, E_2 represent the "activation energies" corresponding to the spin orbit coupling and the antiferromagnetic exchange interaction. This equation adequately describes the spin−orbit coupling, which results in a splitting between discrete levels. It is in excellent agreement with the experimental data obtained in the present work (Figure 3). The obtained values of $A + B = 10.2\ \mathrm{cm^3\ K\ mol^{-1}}$ and $E_1/k = +64.1$ K (using a least-squares fitting method) are consistent with those obtained from the Curie-Weiss law in the high temperature range ($C \sim 9.8\ \mathrm{cm^3\ K\ mol^{-1}}$) and for the effect of spin−orbit coupling and site distortion (E_1/k of the order of +100 K).[9,19] As for the value found for the antiferromagnetic exchange interaction, it is weak but significant ($E_2/k = 2.38$ K), which agrees with a ferrimagnetic like behavior at lower temperature.

To further investigate the phase transformation at low temperature, the ac magnetic measurements were performed for **1** (Figure S4, Supporting Information), only one peak at ~3.2 K is observed for the real part of ac susceptibility (χ'), and these two peaks have the corresponding peaks in the imaginary part of ac susceptibility (χ''), which become nonzero at 4 K, to reach a first maximum at 3.2 K and a second one at 2 K. Furthermore, an small frequency dependence is observed for all of the peaks found in the ac susceptibility data for the **1**, which can be an indication of a slight degree of spin-glass behavior.[20] This is also consistent with the presence of the bifurcation point between the FCM/ZFCM curves below 3.2 K (Figure S5, Supporting Information). The empirical factor $f = |\theta/T_N| = 7.7$ ($T_N = 3.2$ K defined by ac susceptibility, see below) is less than 10, and the f value

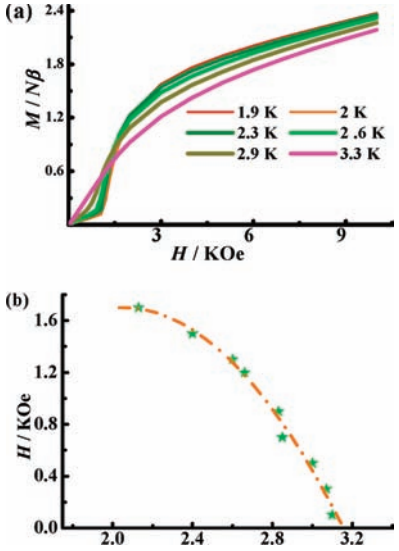

Figure 4. (a) $M(H)$ of **1** measured at different temperatures and their derivatives shown in the inset. (b) The $H-T$ magnetic phase diagram for **1**. The stars is from the $M(T)$ curves, and the line is guide for the eye.

is approximate to triangular $Co^{II}_3(\mu_3\text{-OH})$ based two-dimensional compound ($f = 7.3$),[11c] indicating a moderate geometric frustration presented in this system, which is expected for the magnetic exchange lattice of **1** constructed by distortion of Kagomé lattice (Figure 2). In addition, it should be pointed out that the local antiferromagnetic exchange in the distortion of Kagomé lattice is not equilateral. Thus, this moderate geometric frustrate lattice as well as the local disorder mainly respond to the spin-glassy behavior of **1**.[12,13]

To complement our studies on this system, we carried out isothermal magnetization experiments at low temperatures. Interestingly, the central portion of the loop at 2 K show an obvious *S*-type shape (Figure 3 inset), indicating a metamagnetic transition. The magnetization of 5.42 Nβ at 7 T is below the normally observed value of 9 $N\beta$ for an isotropic high spin Co_3^{II}. This is consistent with weak ferromagnetism because of ferrimagnetic-like arrangement of the total spin moments. Such behavior further confirmed by a series of low-temperature $M(T)$ measurements (Figure 4a).[6−8] The critical field H_c for the metamagnetic transition at 2 K is deduced to be about 1.2 kOe (Figure S6, Supporting Information).[2−8] These observations prompted delicate $M(H)$ measurements in order to obtain the $H-T$ magnetic phase diagram for **1**. The *S*-shape abnormality of the curve becomes less pronounced upon increasing the temperature (Figure S7, Supporting Information). The differentials of these curves show peaks that shift to lower fields as the temperature increases. The magnetic phase diagram for both regimes is shown in Figure 4c and is also established for reported $[Co_3(C_6H(COO)_5)(OH)(H_2O)_3]$, etc.[8] The plot gives an estimated critical temperature of $T_N = 3.2$ K.[19]

The magnetostructure of **1** is rather complicated (Figure 2) and can hardly be quantitatively studied by simple analytical expressions. It is noted that two kinds of magnetic pathways can be considered,[19] that is, intralayer and interlayer (Figure 2). In each Kagomé-type layer, because of the triangular alignment of these antiferromagnetic interactions involving many magnetic bridges

(18) (a) Miller, J. S.; Drillon, M. *Magnetism to Materials V*; Willey-VCH: Weinheim, Germany, 2005, pp 347−377. (b) Rueff, J.-M.; Paulsen, C.; Souletie, J.; Drillon, M.; Rabu, P. *J. Solid State Chem.* **2005**, *7*, 431. (c) Rueff, J.-M.; Masciocchi, N.; Rabu, P.; Sironi, A.; Skoulios, A. *Chem. Eur. J.* **2002**, *8*, 1813.

(19) Kahn, O. *Molecular Magnetism*; VCH Publishers: New York, 1993; Carlin, R. L. *Magnetochemistry*; Springer-Verlag: Berlin, Germany, 1986.

(20) (a) Mydosh, J. A. *Spin Glasses*; Taylor and Francis: Washington, DC, 1993; Chapter 1. (b) Coronado, E.; Galán-Mascrós, J. R. Martí-Gastaldo, C.; Ribera, A.; Palacios, E.; Castro, M.; Burriel R. *Inorg. Chem.* **2008**, *47*, 9103 and references therein.

with different amplitudes, the weak ferromagnetism due to ferrimagnetic arrangement is the characteristic of the compound **1**, and leading obvious noncompensated moments. Furthermore, the interlayer AF coupling mediated by the long, covalent aryl ina-bridges is expected to be weak but required for magnetic ordering.[19] On the other hand, purely electrostatic dipolar interactions between the layers can be less effective at such a distance.[8c] Obviously, **1** exhibits a strong magneto-structural anisotropy, from single-ion anisotropy to anisotropic clusters, layers, and the final 3D pillared layers structure. Consequently, multiple metal sites, inter- and intralayer exchange, spin− orbit coupling, and geometrical frustration of the 3D motif, which result in a typical metamagnet under applied field.

Conclusion

In summary, we report the first example of cobalt based, typical metamagnet with pillared Kagomé-like trilayer 3D motif. Evidently, 3-hydroxypicolinate utilized here, has the potential to generate novel frameworks with promising structural features and properties. Furthermore, these results strongly justify further work on above mixed pyridyl-type monocarboxylate systems with long pillar coligands and other transition metals may lead to even more interesting and metamagnetic pillared layer frameworks.

Acknowledgment. This work was supported by NSFC (No. 20871034), GXSFC (No.0832001Z), the Program for New Century Excellent Talents in University of the Ministry of Education China (NCET-07-217), and the Project of Ten, Hundred, Thousand Distinguished Talents in New Century of Guangxi (No. 2006201), as well as Fok Ying Tung Education Foundation (111014). We also thank the reviewers for their helpful comments.

Supporting Information Available: Crystallographic data (CIF), graphics showing coordination modes, hydrogen bonding, non-interpentrating topology, χ_m^{-1} versus T, ac susceptibility, magnetization curves, and dM/dH versus H, $M(T)$ of **1**, and tables showing hydrogen bond lengths and angles, This material is available free of charge via the Internet at http://pubs.acs.org. CCDC reference number 724446 for compound **1**, contains the supplementary crystallographic data for this paper. These data can be obtained free of charge via www.ccdc.cam.ac.uk/conts/retrieving.html (or from the Cambridge Crystallographic Centre, 12 Union Road, Cambridge CB21EZ, UK; Fax: (+44)1223− 336− 033; or e-mail: deposit@ccdc.cam.ac.uk).